Supporting Information

Mechanism of CO Intercalation through the Graphene/Ni(111) Interface and Effect of Doping

Daniele Perilli,[1] Sara Fiori,[2,3] Mirco Panighel, [2] Hongsheng Liu,[1,4] Cinzia Cepek,[2] Maria Peressi,[3] Giovanni Comelli,[2,3] Cristina Africh[2*] and Cristiana Di Valentin[1,*]

[*] Corresponding authors: africh@iom.cnr.it, cristiana.divalentin@unimib.it

[1] Dipartimento di Scienza dei Materiali, Università di Milano-Bicocca,
via R. Cozzi 55, I-20125 Milano, Italy
[2] CNR-IOM, Laboratorio TASC, S.S. 14 Km 163.5, Basovizza, 34149, Trieste, Italy
[3] Department of Physics, University of Trieste, via A. Valerio 2, 34127, Trieste, Italy
[4] Laboratory of Materials Modification by Laser, Ion and Electron Beams,
Dalian University of Technology, Ministry of Education, Dalian 116024, China

1. Computational Details

Density Functional Theory (DFT) calculations were performed using the plane-wave-based Quantum ESPRESSO package (QE).[1,2] The ultrasoft pseudopotentials[3] were adopted to describe the electron-ion interaction with Ni (3d, 4s), C (2s, 2p), O (2s, 2p), N (2s, 2p), and H (1s), treated as valence electrons. Energy cutoffs of 30 Ry and 240 Ry (for kinetic energy and charge density expansion, respectively) were adopted for all calculations. The Perdew-Burke-Ernzerhof functional (PBE) was used for electron exchange-correlation.[4] To properly describe the Gr/Ni interaction, semiempirical corrections accounting for the van der Waals interactions were included with the DFT-D2 formalism.[5] Spin polarization was always included.

For the simulation of nickel(111)-supported epitaxial graphene interfaces (Gr/Ni) in the top-fcc registry, (2√7 × 2√7) and (8 × 8) supercells were used for pristine and defective graphene, respectively.

The geometry relaxation of all considered systems was performed only at Γ point, followed by a single self-consistent field (SCF) cycle calculation with a 2 × 2 × 1 Monkhorst-Pack k-points mesh[6] to get more accurate total energies.

The Ni(111) surface was modeled by a three-layer slab with a bottom layer fixed to the bulk positions during the geometry relaxation to mimic a semi-infinite solid. To avoid interactions between adjacent periodic images, a vacuum space of about 15 Å in the direction perpendicular to the surface was used.

The Climbing Image−Nudged Elastic Band (CI−NEB) method[7] was employed to simulate the CO diffusion process at the Gr/Ni interface, generating the minimum energy path of the reaction step and an evaluation of the energy barrier.

STM simulations were performed using the Tersoff-Hamann approach,[8] according to which the tunneling current is proportional to the energy-integrated Local Density of States (ILDOS). Ball-and-stick models and STM images were rendered with XCrySDen[9] and Gwyddion[10] software, respectively.

The adsorption energy (ΔE_{ads}), as normalized by the number of CO molecules (n), was calculated as follows:

$$\Delta E_{ads} = (E_{nCO/system} - nE_{CO} - E_{system})/n$$

where $E_{nCO/system}$ is the total energy of the system (Gr/Ni or 4VG-6H or 4VG-3CO or 4VG-6N) with n adsorbed CO molecules, E_{nCO} is the total energy of n isolated CO molecules in the gas phase, and E_{system} is the total energy of the optimized system without any adsorbed CO molecule.

In the following, we define the contributions for the energy decomposition analysis, as shown in Figure 5 and reported in Table 1:

$$\Delta E_{decoupl} = [(E_{4VG\text{-}6N,dist} - E_{4VG\text{-}6N\text{-}fs,dist} - E_{Ni,dist}) - (E_{4VG\text{-}6N} - E_{4VG\text{-}6N\text{-}fs} - E_{Ni})]/n$$

where $E_{4VG\text{-}6N,dist}$, $E_{4VG\text{-}6N\text{-}fs,dist}$, and $E_{Ni,dist}$ are the total energies of Ni-supported 4VG-6N, free-standing 4VG-6N, and Ni substrate, respectively, in the optimized geometry for nCO/4VG-6N, whereas $E_{4VG\text{-}6N}$, $E_{4VG\text{-}6N\text{-}fs}$, and E_{Ni} are the total energies of Ni-supported 4VG-6N, free-standing 4VG-6N, and Ni substrate, respectively, in the optimized geometry of 4VG-6N;

$$\Delta E_{dist} = [(E_{nCO,dist} - E_{nCO}) + (E_{4VG\text{-}6N\text{-}fs,dist} - E_{4VG\text{-}6N\text{-}fs}) + (E_{Ni,dist} - E_{Ni})]/n$$

where $E_{nCO,dist}$ and E_{nCO} are the total energies of n CO molecules in the optimized geometry of nCO/4VG-6N and isolated in the gas-phase, respectively;

$$\Delta E_{bind} = (E_{nCO/4VG\text{-}6N} - E_{nCO,dist} - E_{4VG\text{-}6N,dist})/n$$

where $E_{nCO/4VG\text{-}6N}$ is the total energy of nCO/4VG-6N in its optimized geometry; n is the number of adsorbed CO molecules.

2. Experimental Details

Pristine Gr and N-Gr layers were prepared in a UHV chamber with a base pressure of ~2×10^{-10} mbar. The Ni(111) single crystals were cleaned by several cycles of Ar^+ sputtering at 1.5 kV at room temperature (RT) and annealing at 700 °C, for a few minutes. For the N-Gr growth, a N-doped Ni(111) crystal was used (for the preparation details see Ref. 11). Standard Gr growth was performed in UHV by low-pressure CVD, using ethylene (C_2H_4) as precursor. Low energy electron diffraction (LEED) and STM characterization was performed in UHV in order to assess the quality and homogeneity of the as-grown Gr sample.

CO reactivity experiments have been carried out *in-situ*, in a home-made high-pressure cell inside a small chamber, connected to the experimental setup through a gate valve and kept in high vacuum (~10^{-9} mbar). STM measurements were performed in UHV at room temperature with an Omicron variable-temperature (VT) STM. All topographic images were acquired in constant-current mode. STM images were analyzed with the Gwyddion software package[10], after applying moderate noise filtering. Crystallographic orientation of the images was determined by analyzing the epitaxial structure formed by pristine Gr on the Ni(111) surface, as described in Ref. 12. XPS measurements were performed at a base pressure in the range of 10^{-9} mbar. All the spectra were collected at RT in normal emission geometry using a hemispherical electron energy analyser and a conventional Mg

$K_{\alpha 1,2}$ (1253.6 eV) X-ray source, with an overall experimental energy resolution of ~0.8 eV. All binding energies were calibrated by measuring the Fermi level. The spectra are normalized to the incident photon flux and analysed by performing a non-linear mean square fit of the data. We used a Shirley background and reproduced the C 1s photoemission peacks using asymmetric Doniach-Sunjic lineshapes.

3. Supplementary Figures

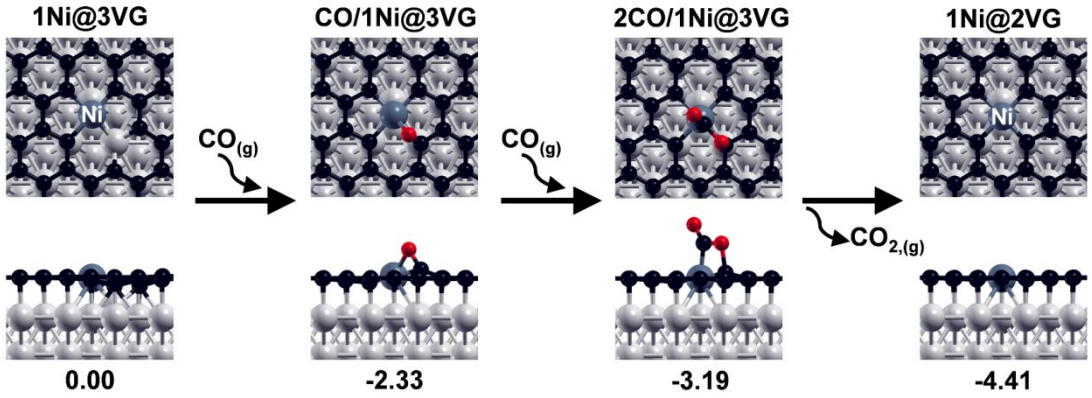

Figure S1. Top and side views of the intermediates along the CO reaction path on the most common defect in pristine Gr/Ni: a tri-atomic C vacancy with a trapped Ni adatom (1Ni@3VG). The reaction energies (in eV) are reported below each structure. Color coding: Ni atoms in grey, Ni adatom (labelled) in dark grey, C atoms in black, O atoms in red.

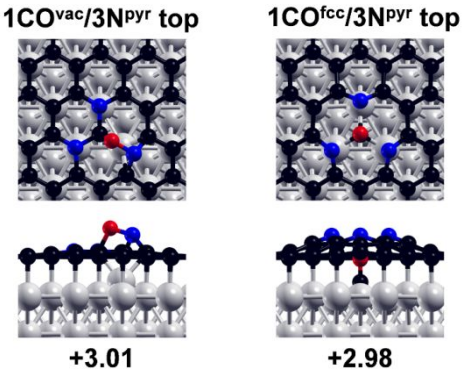

Figure S2. Top and side views of two CO adsorption configurations on the most common defect of N-Gr/Ni: three pyridinic nitrogen atoms in top position ($3N^{pyr}$ top). The adsorption energies (in eV) are reported below each structure. Color coding: Ni atoms in grey, C atoms in black, O atoms in red, N atoms in blue.

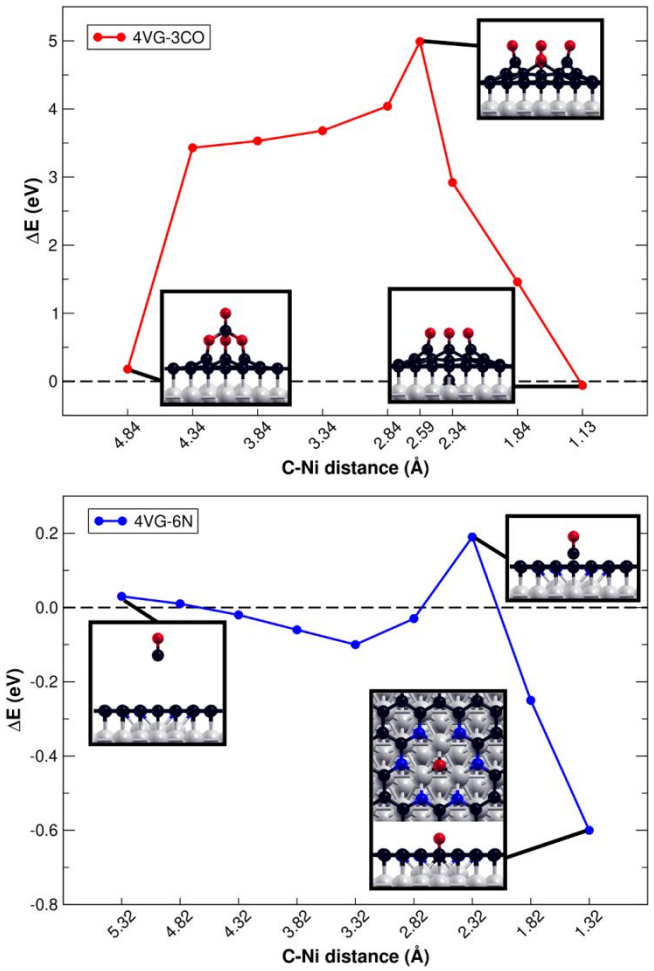

Figure S3. Energy profile for the adsorption step of the first CO molecule as a function of the CO-Ni distance (measured at the position of the C atom in the molecule) on the 4VG-3CO (top panel) and 4VG-6N (bottom panel) models. Color coding: Ni atoms in grey, C atoms in black, O atoms in red, N atoms in blue.

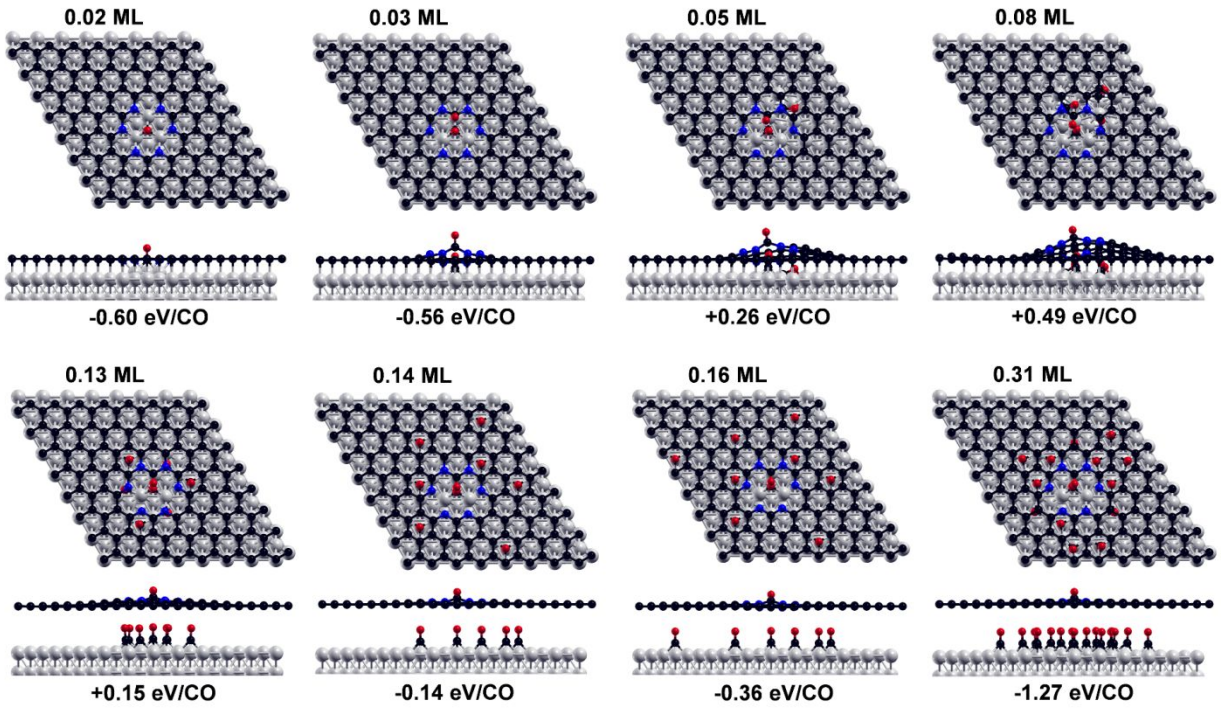

Figure S4. Top and side views of the intermediates of the CO intercalation process on 4VG-6N (as shown in Figure 3d). The adsorption energies (in eV), normalized to the number of CO molecules, are reported below each structure. Color coding: Ni atoms in grey, C atoms in black, O atoms in red, N atoms in blue.

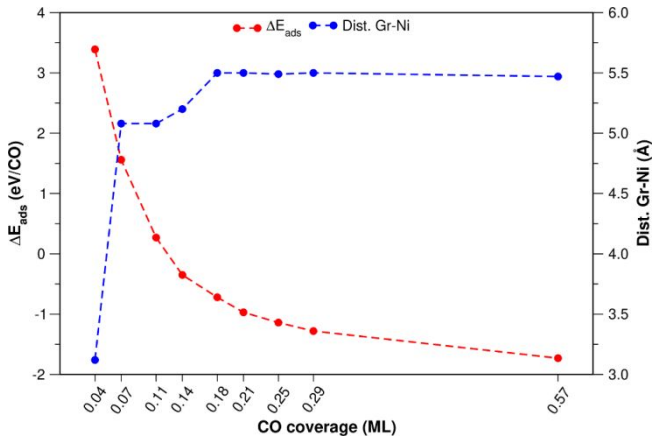

Figure S5. Energy profile (normalized by the number of CO molecules) and Gr-Ni vertical distance (in Å, averaged on all the Ni atoms of the first layer and on all the C atoms of graphene) for the CO adsorption as a function of the CO coverage at the interface between defect-free Gr and Ni(111) surface (red and blue line, respectively).

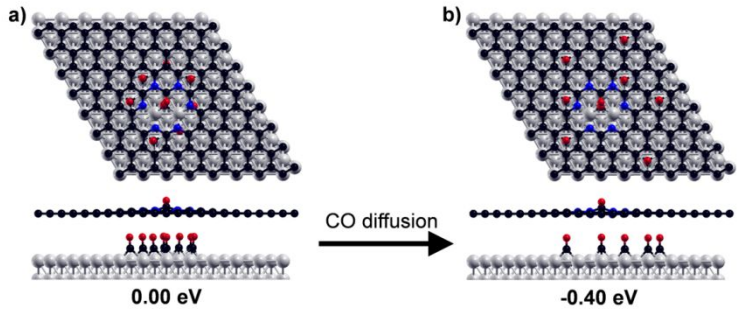

Figure S6. Top and side views of two different configurations at a CO coverage of 0.14 ML for 4VG-6N model. The two structures differ for the distribution of the intercalated CO molecules: a) close to the hole edges and b) most widespread. The relative energy (in unit of eV) with respect to the model (a) is reported below each configuration. Color coding: Ni atoms in grey, C atoms in black, O atoms in red, N atoms in blue.

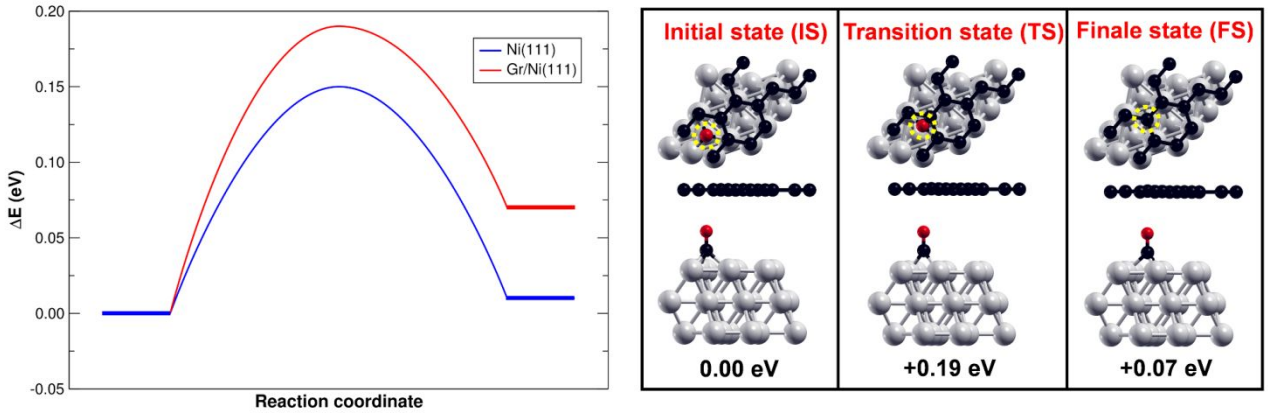

Figure S7. Energy profile (as obtained through a CI-NEB calculation) of the CO diffusion at a coverage of 0.14 ML for bare (red line) and Gr-covered (blue line) Ni (111) surface (left panel). Top and side views of the initial (hcp), transition (bridge), and final (fcc) configurations along the CO diffusion path of the Gr-covered system (right panel). The relative energy (in eV) with respect to the initial state is reported below each configuration. The position of the CO molecule is indicated by a dotted yellow circle in the top representation. Color coding: Ni atoms in grey, C atoms in black, O atoms in red.

4. Supplementary Table

Table S1 Energy contributions of the energy decomposition analysis for CO adsorption on 4VG-6N of distortion (positive, ΔE_{dist}), decoupling (positive, ΔE_{decoup}) and of binding (negative, ΔE_{bind}) to the total adsorption energy ($\Delta E_{ads\text{-}tot}$) for all CO molecules, at different CO coverages. The energy contributions are calculated using as a reference the optimized 4VG-6N interface and isolated CO molecules in the gas-phase.

CO Coverage (ML)	n CO	$\Delta E_{ads\text{-}tot}$ (eV)	ΔE_{dist} (eV)	ΔE_{decoup} (eV)	ΔE_{bind} (eV)
0.03	2	-1.13	+0.86	+1.17	-3.16
0.05	3	+0.79	+4.36	+1.33	-4.90
0.13	8	+1.23	+0.66	+21.3	-20.7
0.14	9	-1.30	+0.34	+21.8	-23.5

References

[1] Giannozzi, P.; Baroni, S.; Bonini, N.; Calandra, M.; Car, R.; Cavazzoni, C.; Ceresoli, D.; Chiarotti, G. L.; Cococcioni, M.; Dabo, I.; et al. Quantum ESPRESSO: a modular and open-source software project for quantum simulations of materials. *J. Phys.: Condens. Matter* **2009**, *21*, 395502.

[2] Giannozzi, P.; Andreussi, O.; Brumme, T.; Bunau, O.; Buongiorno Nardelli, M.; Calandra, M.; Car, R.; Cavazzoni, C.; Ceresoli, D.; Cococcioni, M.; et al. Advanced capabilities for materials modelling with Quantum ESPRESSO. *J. Phys.: Condens. Matter* **2007**, *29*, 465901.

[3] Vanderbilt, D. Soft self-consistent pseudopotentials in a generalized eigenvalue formalism. *Phys. Rev. B* **1990**, *41*, 7892.

[4] Perdew, J. P.; Burke, K.; Ernzerhof, M. Generalized gradient approximation made simple. *Phys. Rev. Lett.* **1996**, *77*, 3865.

[5] Grimme, S. Semiempirical GGA-type density functional constructed with a long-range dispersion correction. *J. Comput. Chem.* **2006**, *27*, 1787–1799.

[6] Monkhorst, H. J.; Pack, J. D. Special points for Brillouin-zone integrations. *Phys. Rev. B* **1976**, *13*, 5188.

[7] Henkelman, G.; Uberuaga, B. P.; Jónsson, H. A climbing image nudged elastic band method for finding saddle points and minimum energy paths. *J. Chem. Phys.* **2000**, *113*, 9901-9904.

[8] Tersoff, J.; Hamann, D. R. Theory of the scanning tunneling microscope. *Phys. Rev. B* **1985**, *31*, 805.

[9] Kokalj, A. XCrySDen−a new program for displaying crystalline structures and electron densities. *J. Mol. Graph. Model.* **1999**, *17*, 176-179.

[10] Nečas, D.; Klapetek, P. Gwyddion: an open-source software for SPM data analysis. *Open Phys.* **2012**, *10*, 181–188.

[11] Fiori, S.; Perilli, D.; Panighel, M.; Cepek, C.; Ugolotti, A.; Sala, A.; Liu, H.; Comelli, G.; Di Valentin, C.; Africh, C. “Inside Out” Growth Method for High-Quality Nitrogen-Doped Graphene. *Carbon* **2020**, in press (http://arxiv.org/abs/2009.09789).

[12] Patera, L. L.; Africh, C.; Weatherup, R. S.; Blume, R.; Bhardwaj, S.; Castellarin-Cudia, C.; Knop-Gericke, S.; Schloegl, R.; Comelli, G.; Hofmann, S.; Cepek, C. In situ observations of the atomistic mechanisms of Ni catalyzed low temperature graphene growth. *ACS Nano* **2013**, *7*, 7901-7912.